

The effect of Zn ion substitution on electromagnetic properties of low-temperature fired Z-type hexaferrite

Hongguo Zhang*, Ji Zhou, Yongli Wang, Longtu Li, Zhenxing Yue, Zhilun Gui

State Key Laboratory of New Ceramics and Fine Processing, Department of Materials Science and Engineering, Tsinghua University, Beijing 100084, China

Received 11 November 2001; received in revised form 2 March 2002; accepted 10 April 2002

Abstract

The influence of Zn substitution on the densification, microstructure, lattice parameters and electromagnetic properties of planar Z-type hexaferrites, which have stoichiometric composition of $\text{Ba}_3\text{Co}_{2(10.8-x)}\text{Zn}_{2x}\text{Cu}_{0.4}\text{Fe}_{24}\text{O}_{41}$, were investigated. The results show that the Zn^{2+} substitution has no obvious effect on the densification, but Z-type hexagonal phase can form and demonstrate typical planar anisotropic characteristics of soft magnetic materials ($\sigma_r \leq 6.20$ emu/g) in the range of $x \leq 0.25$. The of lattice parameters of planar a (0.588 nm) and axial c (5.25 nm) remain stable. At the certain temperatures, the sintered hexaferrites with an optimal density of about 4.62 g/cm³ show better electromagnetic properties for $x=0.15$ than the samples without Zn^{2+} incorporation: initial permeability of about 9.0, cut-off frequency of above 800 MHz, resistivity of above 3.20 Ω cm and dielectric constant of less than 35.

© 2002 Elsevier Science Ltd and Techna S.r.l. All rights reserved.

Keywords: C. Magnetic properties; C. Electrical properties; D. Ferrites; E. Functional application

1. Introduction

Recently, UHF (ultra high frequency: from 200 to 1000 MHz) devices have become necessary commercially for application in the surface mounting devices (SMD) [1,2]. Multi-layer chip inductor (MLCI) is one of the most important SMD. By taping ferrites and coating internal electrode pastes, MLCI is produced. Since Ag or Ag–Pd alloy is usually used as electrode pastes, high temperature co-firing causes unexpected lowering of initial permeability due to the interfacial diffusion between the ferrite and electrode paste [3–5]. This interfacial diffusion can be overcome by co-firing at a temperature lower than the melting point of Ag (961 °C). Therefore, low temperature sintered ferrite is strongly demanded. However, the low-temperature fired ferrites usually can not present high performance.

By now, NiZnCu ferrites have been commercially used for MLCI for a few years, but they do suffer from

a fatal disadvantage of low resonant frequency, which is not suitable for the increasing frequency range of MLCI. The so-called Snoek law [6], however, restricts their use below 200 MHz.

Hexaferrites with hexagonal structure have revealed a higher dispersion frequency than that of NiZnCu ferrites due to the magnetic anisotropy. Among those ferrites, Z-type hexaferrite has the highest resonant frequency, presents excellent electromagnetic properties in UHF region, and thus appears to hold considerable promise in the MLCI production [7].

A preliminary study [8] by the present authors has been aimed to improve the magnetic properties of Co_2Z compound by replacing some of the cobalt ions with copper ions according to the formula $\text{Ba}_3\text{Co}_{2(1-x-y)}\text{Zn}_{2x}\text{Cu}_{2y}\text{Fe}_{24}\text{O}_{41}$. The substitution was expected to lower the sintering temperature and increase the initial permeability in UHF region. Moreover, cobalt ions are known to form a solid solution with zinc and copper ions in the stoichiometric range of $y=0.10$ – 0.30 . The best magnetic properties were obtained in the preliminary study at $y=0.20$ for samples sintered at 1100–1150 °C/4 h with $x=0.00$. Even at 600 MHz, its permeability did not decrease as detailed elsewhere [8].

* Corresponding author at present address: Laboratory of Electronic Materials and Devices, Department of Materials Science, University of North Texas, PO Box 305310, Denton, TX 76203, USA.

E-mail address: zhg67320@hotmail.com (H. Zhang).

In the present work, the value of y being fixed at 0.20, an attempt was made to change the zinc content from $x=0.05$ to 0.25 with the hope of increasing initial permeability in the materials. The green compacts were prepared by the usual ceramic route without a magnetic field to avoid the occurrence of preferred orientation of the basal plane for hexagonal ferrites.

2. Experimental procedure

2.1. Sample preparation

The ferrites having stoichiometric compositions of $\text{Ba}_3\text{Co}_{2(0.8-x)}\text{Zn}_{2x}\text{Cu}_{0.4}\text{Fe}_{24}\text{O}_{41}$, where $x=0.05, 0.10, 0.15, 0.20$, and 0.25 , were prepared by the usual ceramic route. The raw materials, BaCO_3 , Co_2O_3 , ZnO , CuO and Fe_2O_3 , of high purity (all $\geq 99.5\%$), were mixed in a ball mill for 4 h. The mixed powders were calcined at $1000\text{--}1050\text{ }^\circ\text{C}/4\text{ h}$ in air, and then milled for 4 h again. The resulted powders were pressed in a stainless-steel die under a pressure of about 4000 N/m^2 with 5 wt.% PVA as binder. The pressed pellets (10 mm outside diameter, 0.5–1.5 mm thickness) and toroidal samples (20 mm outside diameter, 10 mm inside diameter, about 3 mm thickness) were sintered at $1100\text{--}1150\text{ }^\circ\text{C}/4\text{ h}$ in air and then cooled in the furnace. After each sintering experiment, the weights and dimensions of the toroidal samples were measured at room temperature to determine bulk densities.

2.2. Microstructure characteristics

The phase evolution of the calcined powders was analyzed using X-ray diffractometry (XRD). Data collection was carried out using FeK_α radiation at 35 kV and 25 mA in the range of $2\theta=35\text{--}65^\circ$ with a scanning speed of $2^\circ/\text{min}$. Grain size could be calculated by the Scherrer formula.

Scanning electron micrograph (SEM) was carried out to study grain morphology evolution, distribution and average grain size.

2.3. Magnetic property measurements

The DC resistivity of samples at room temperature was measured by HP4140B using silver-paste contacts. HP4191A or HP4291B impedance/materials analyzer from 1 to 1800 MHz measured the frequency properties of ceramic samples.

The change of magnetization (M_s) for Curie-temperature (T_c) and magnetic hysteresis curves were measured at LDJ9600 VSM (vibration sample magnetometer).

3. Results and discussion

3.1. Variation of structural properties

3.1.1. Densification

The range of substituting content of zinc ions of 0.05–0.25 is determined according to Ref. [9]. When $(x+y)\geq 0.80$, Z-type hexaferrite will change its property from planar to axial anisotropy, and thus not possesses soft magnetic properties.

By incorporating Zn into hexaferrites, which have the stoichiometric composition of $\text{Ba}_3\text{Co}_{2(0.8-x)}\text{Zn}_{2x}\text{Cu}_{0.4}\text{Fe}_{24}\text{O}_{41}$, no obvious variation in density can be obtained. This means the incorporation of Zn do not generate great effect on the densification of substituted Co_2Z ferrite. Nevertheless, the densification of substituted Co_2Z ferrite depends on the change of Cu content and sintering temperature [8]. The average density of hexaferrites with $x=0.05\text{--}0.25$ at $1100\text{--}1150\text{ }^\circ\text{C}/4\text{ h}$ was 4.62 g/cm^3 .

It is known that the melting point of CuO and ZnO is 1026 and $1530\text{ }^\circ\text{C}$ respectively. So, the densification of substituted hexaferrites at relatively low temperatures may be the formation of a new solid solution with appropriate content CuO. Moreover, appropriate segregation of CuO not only lowers the sintering temperature, but also improves grain morphology, distribution of inner pores as described by Burke [10]. Due to the existence of liquid CuO around ferrite grains, it will promote the reaction with other oxides, atom transportation and diffusion among different grains during low temperature sintering, and thus improve the consequent densification.

3.1.2. Phase identification

Fig. 1 shows X-ray diffraction analytical spectra of the samples sintered at $1100\text{--}1150\text{ }^\circ\text{C}/4\text{ h}$. When the same thermal treatment was used, the samples exhibit typical Z-type phase structure. Fig. 2 plots the variation of magnetization of different samples and also demonstrates the typical characteristics of soft magnetic ferrites; the measured remnant magnetization is only 6.12–7.71 emu/g. However, the samples possibly contain small amount of Y ($\text{Ba}_2\text{Co}_2\text{Fe}_{12}\text{O}_{22}$) phase, which was not detected and co-existed with Z-type phase according to Pullar et al.'s report [11,12].

3.1.3. Microstructure characterization

By introducing a relatively small number of Zn^{2+} , no obvious change for the microstructure of Z-type hexaferrites can be observed. Fig. 3 demonstrates SEM pictures of the modified samples sintered at different temperatures for 4 h respectively. Just like Cu modified hexaferrites [8], small, homogeneous and rod-like grains (platelet grains of $20\text{ }\mu\text{m}$ for pure Co_2Z) for Zn substituted Z-type ferrite (the average grain size: $10\text{--}15\text{ }\mu\text{m}$)

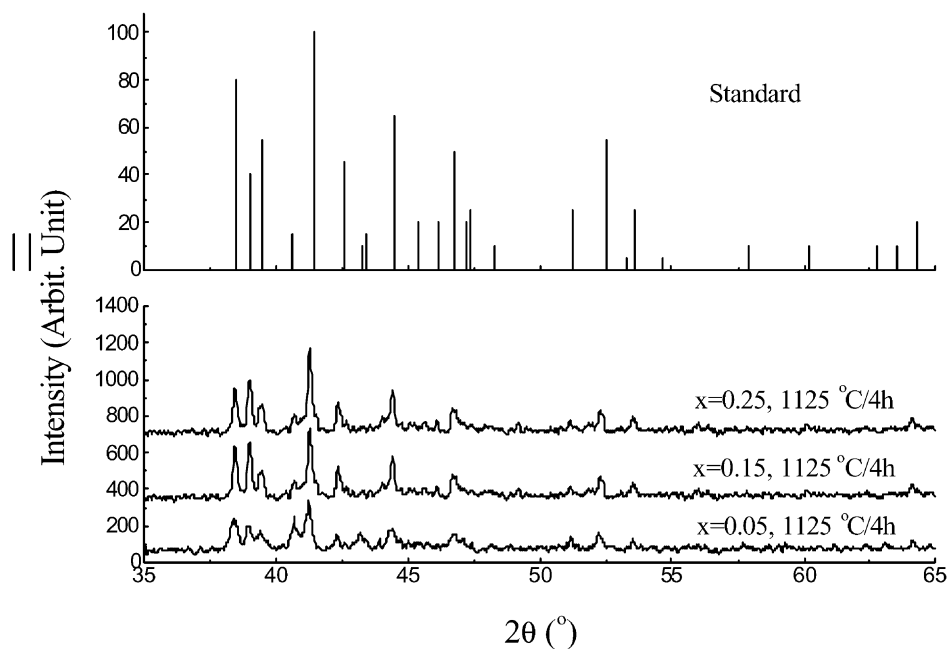


Fig. 1. XRD spectra of Zn modified Z-type hexaferrite.

were observed. This indicates that the grain growth and pores in the grains is not affected by Zn incorporation, but mainly depends on the Cu content and the sintering temperature.

Co^{2+} is one of the strong magnetic crystalline anisotropic ions, but Zn^{2+} and Cu^{2+} are not [6,9]. Once Zn^{2+} enter into the lattice of Z-type phase, the degree of anisotropy of Z-type hexaferrite decreases, which leads to the variation of crystallite structure: transition from planar to axial anisotropy [9]. That rod-like grains become more homogeneously small and little porous implies that grain growth mainly proceeds in three-dimensional manner, still prefers in the plane perpendicular to the *C*-axis.

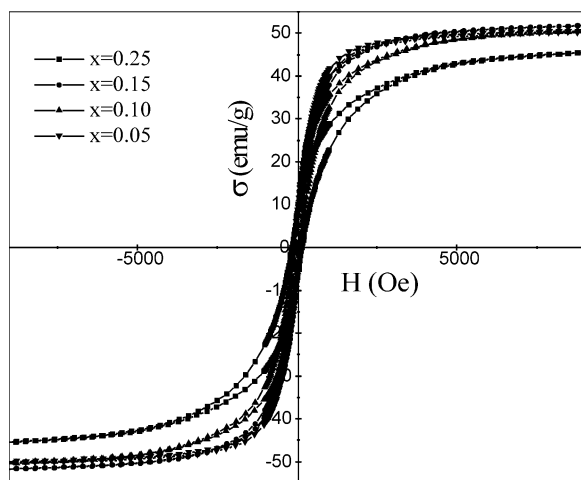


Fig. 2. Magnetic hysteresis curves of Zn substituted Z-type hexaferrites sintered at 1125 °C/4 h.

Fig. 4 gives the variation of lattice parameters for Zn substituted Z-type hexaferrites. The crystalline parameters, which was calculated by Scherrer formula, reserves stable: planar *a* of about 0.588 nm and axial *c* of about 5.225 nm respectively. It is obvious that the incorporation of zinc has little effect on crystalline structure of Cu modified hexaferrites.

3.2. Magnetic properties of sintered samples

Ceramic samples thus achieved from the composition $x=0.15$ sintered at 1125 °C/4 h presents good magnetic properties as following: the initial permeability of more than 9.0, and cutoff frequency of above 800 MHz, seen in Fig. 6 and Table 1. It can be observed that there was an obvious increase for the initial permeability compared with that of samples without Zn substitution. Nevertheless, the initial permeability is lower than that of pure Co_2Z ferrite (Fig. 5) [8].

As we all know, the magnetism of soft hexaferrites results from spin rotation and domain walls motion. For polycrystalline hexaferrites, the initial permeability mainly depends on the grain size, sintering density and magnetization and, increases with the increase of the grain size, density and magnetization [10]. As seen in Table 1 and observed in Fig. 2, although the saturation magnetization is lower than that of pure Co_2Z , it is higher than that of Cu modified samples, i.e. $\text{Ba}_3\text{Co}_{1.6}\text{Cu}_{0.4}\text{Fe}_{24}\text{O}_{41}$.

The effect of Zn ion substitution on the initial permeability (measured at room temperature) is given in Fig. 6. Fig. 6 shows that the value of the initial permeability increases as Zn^{2+} substitution increases. This

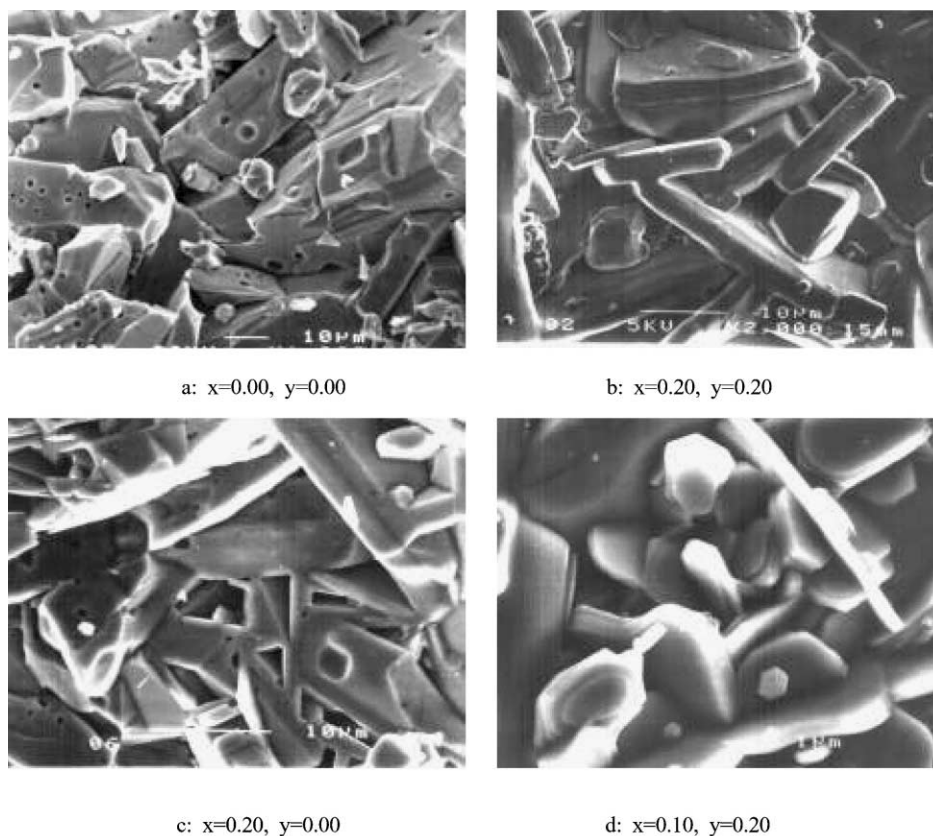


Fig. 3. SEM micrographs of the sintered specimens.

may be related to the increase in the replacement of non-magnetic Zn ions to magnetic Co ions. It is suggested that the superexchange interaction between the magnetic ions in different sublattices (which results in the parallel alignment magnetic vector to the direction perpendicular to C-axis) is stronger than that within the same sublattices [6,9]. The strength of this exchange interaction increases when a magnetic (Co^{2+}) ion is replaced by non-magnetic (Zn^{2+}) ion [9]. This leads to a stability of the parallel alignment between ions and the anisotropy tends to be perpendicular to c axis. This explains the increase in the initial permeability as Zn ion replacement to Co ion increases. However, when the replacement content of Zn is higher than a certain value, the strength of this exchange interaction decreases according to Braun's report because Zn^{2+} is anti-ferromagnetic but Cu^{2+} and Co^{2+} are ferromagnetic [9]. This also explains why Zn^{2+} molar ratio is chosen as $x \leq 0.25$.

On the other hand, the decrease in the initial permeability for Zn substituted Z-type hexaferrite is possibly due to the suppressed grain growth due to the presentation of Cu^{2+} and the low sintering temperature, which commonly occur in spinel ferrites [13].

Furthermore, the decrease of the initial permeability can also be correlated with the microstructure of the

ferrite. Zn ions that enter into the lattice, due to their electronic configuration, will distort the lattice or crystalline field, generating an internal stress that will hinder the domain wall motion or spin rotation and, as a consequence, the permeability will decrease.

In spite of the above-mentioned, Cu ions segregate at the grain boundary during the sintering process will diffuse into the grain boundaries. In this case, a part of CuO act as a sintering aid and exist in the liquid-phase, which is considered beneficial to the synthesis of Z-type hexaferrite with high density and facilitates the growth of small grains with inner pores [14]. In consequence, the structure of the resulted hexaferrite presents homogeneous grain, a high density and a small number of intragranular pores. Therefore, a little increase in the initial permeability will be obtained for the substituted hexaferrites.

3.3. The effect of Zn^{2+} substitution on electrical properties

As an important requirement for MLCI, the electrical resistivity is higher than $3.27 \times 10^7 \Omega\text{-cm}$ at about $x=0.05$ (Fig. 6). Dielectric constant is less than 35 at below 500 MHz (Fig. 7 and Table 1).

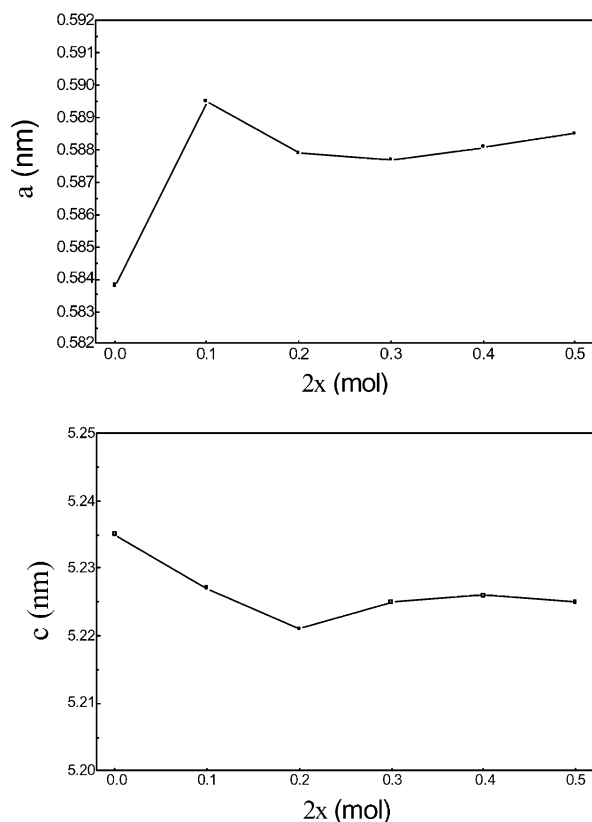


Fig. 4. Compositional variation of lattice constants in the $\text{Ba}_3\text{Co}_{2(0.8-x)}\text{Zn}_{2x}\text{Cu}_{0.4}\text{Fe}_{24}\text{O}_{41}$ system.

It has been reported that the magnetic Co^{2+} ion preferentially occupies the tetrahedral sites (A) [15,16]. Magnetic Fe ions partially occupy A-sites as well as octahedral sites (B) [6]. Non-magnetic Zn^{2+} ions strongly prefer the A-sites [17,18]. As the Zn^{2+} ion substitution increases preferably in A-sites, some of Fe ions at A-sites will migrate to B-sites. As a consequence, the chance of electron generation decrease as the prob-

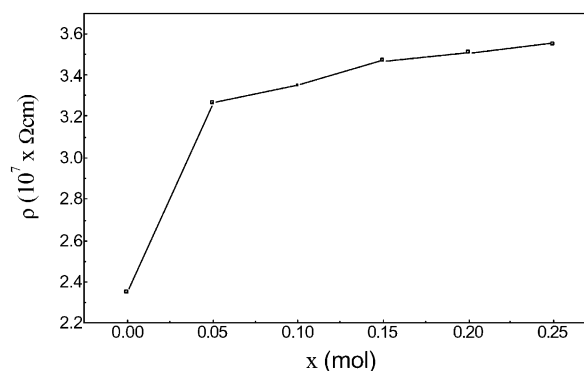
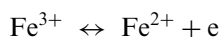


Fig. 6. Compositional variation of DC resistivity in the $\text{Ba}_3\text{Co}_{2(0.8-x)}\text{Zn}_{2x}\text{Cu}_{0.4}\text{Fe}_{24}\text{O}_{41}$ system.

ability of Fe ion migration and the following reaction decrease:



Furthermore, due to the low sintering temperature, the probability of electron hopping, Fe^{2+} formation and Fe ion diffusion to B-sites decrease greatly, so this leads to a increase in resistivity for Zn substituted samples.

According to Koops theory for most ferrites [19], the dielectric constant is directly proportional to the root mean square of the resistivity reciprocal; therefore the dielectric constant decreases for the Zn substituted hexaferrites.

3.4. Discussion

Fig. 8 shows the variation of magnetization as a function of temperatures. The Curie temperatures (T_c) for the samples are listed in Table 1. It can be seen that T_c decreases as Zn^{2+} ion substitution increase. This may be attributed to the replacement of non-magnetic

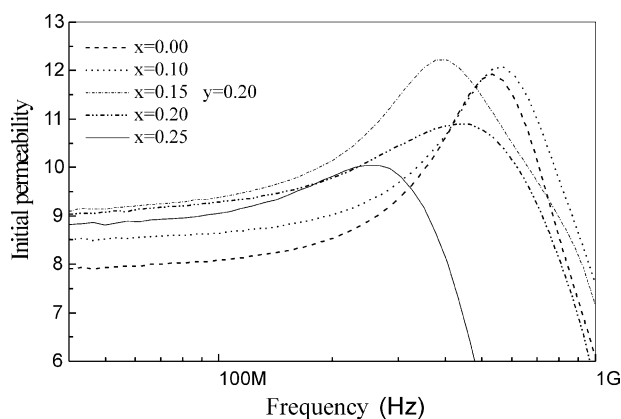


Fig. 5. Frequency dependence of initial permeability for specimens sintered at 1100–1150 °C/4 h.

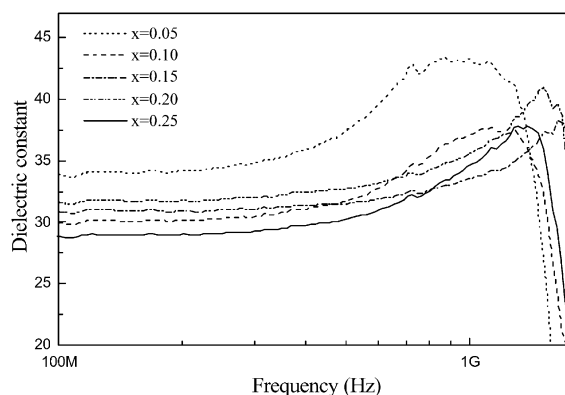


Fig. 7. Frequency dependence of dielectric constant for specimens sintered at 1100–1150 °C/4 h.

Table 1

Compositional variation of lattice constant, resistivity, dielectric constant, saturation magnetization and Curie temperature (T_c) in the $\text{Ba}_3\text{Co}_{2(0.8-x)}\text{Zn}_{2x}\text{Cu}_{0.4}\text{Fe}_{24}\text{O}_{41}$ system

	a (nm)	c (nm)	ρ ($\times 10^7 \Omega \text{ cm}$) (25 °C)	ε (≤ 800 MHz)	σ_s (emu/g)	T_c (K)
$x=0.05$	0.587	5.221	3.27	34	50	625
$x=0.10$	0.583	5.228	3.35	30	52	600
$x=0.15$	0.580	5.235	3.47	31	53	550
$x=0.20$	0.579	5.236	3.51	32	46	450

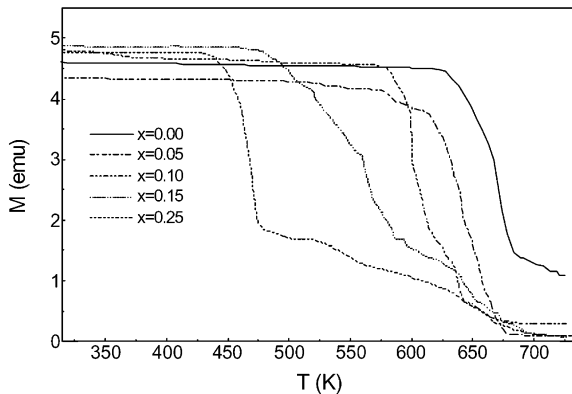


Fig. 8. The variation of magnetization for Curie temperature (T_c).

Zn^{2+} to magnetic Co^{2+} ions, which will affect the magnetic order and reduce the exchange interaction; namely makes the magnetic state transmit easily from ferromagnetic to out-of-order paramagnetic alignment. However, the decrease of T_c will damage the substituted Z-type hexaferrite in the application of MLCI production.

Simultaneously incorporating Zn and Cu into pure Co_2Z , substituted Z-type hexaferrite with planar hexagonal structure and excellent electromagnetic properties could be obtained at relatively low temperatures. It has exhibited great potentiality in the fabrication of MLCI when co-fired with cheap interconnecting materials (Ag, Ni et al.) and Bi_2O_3 additive et al. [20].

4. Conclusions

1. The substitution of Zn in Z-type planar hexaferrites cannot generate obvious effect on the densification, grain growth, and the sintering temperature, but can improve the electromagnetic properties of Z-type hexaferrites, compared with sole Cu modification.
2. The optimum content of Zn is appreciated to be $x=0.15$, which was sufficient to yield good magnetic properties as following: 9.0 of initial permeability, 53.34 emu/g of magnetization, 1.0 GHz of resonant frequency, $3.47 \times 10^7 \Omega \cdot \text{cm}$ of resistivity at room temperature, 31 of dielectric constant (≤ 400 MHz) and about 550 K of T_c .
3. The development of low sintering temperature Z-type modified hexaferrites will enable the ceramics to be co-fired with less expensive contact materials (Ag et al.) in production of MLCI. The relative mechanisms associated with modification and that generates these effects are currently under further investigation.

Acknowledgements

The authors were indebted to the financial support from the High Technology and Development Project of the PR China (Grant: 715-Z33-006-0050), National Natural Science Foundation of PR China (Grant: 59995523), and the Ceramic Technology Center, Motorola, Inc., USA. We would like to thank Dr. Micheal and Q. Manuel in University of North Texas for their helpful discussion.

References

- [1] H. Winard, Electronic Design, March 13 (1986) 41.
- [2] H.M. Sung, C.J. Chen, W.S. Ko, H.C. Lin, IEEE Trans on Magn. 30 (6) (1994) 4906.
- [3] T. Nakamura, Y. Okano, Y. Miura, J. Mater. Sci. 33 (4) (1998) 1091.
- [4] J.Y. Hsu, W.S. Ko, H.D. Shen, C.J. Chen, IEEE Trans on Magn. 30 (6) (1994) 4875.
- [5] J.H. Nam, H.H. Jung, J.Y. Shin, J.H. Oh, IEEE Trans on Magn. 31 (6) (1995) 3985.
- [6] J. Smit, H.H.J. Wijn, Ferrite, Philips Technical Library, Eindhoven, Netherlands, 1959, p. 278.
- [7] O. Kimura, M. Matsumoto, M. Sakakura, J. Am. Ceram. Soc. 78 (10) (1995) 2857.
- [8] H.G. Zhang, L.T. Li, J. Zhou. IEEE Trans on Magn. 38 (4) (2002) 1797–1802.

- [9] P.B. Braun, Philips Res. Rep. 12 (1957) 491.
- [10] J.E. Burke, in: W. D. Kingery (Ed.), *Ceramic Fabrication Processes*, Wiley, New York, 1958, p. 120.
- [11] R.C. Pullar, S.G. Appleton, A.K. Bhattacharya, J. Magn. Magn. Mater. 186 (1998) 313.
- [12] D. Autisser, A. Podembski, C. Jacquiod, J. Phys. IV France 7 (1997) C1–409.
- [13] P. Allegri, D. Autissier, T. Taffary, Key Eng. Mater. 132–136 (1997) 1424.
- [14] H. Rikukawa, IEEE Trans. on Magn. 18 (6) (1982) 1535.
- [15] G. Joshi, S. Deshpande, S.R. Sawant, Solid State Commun. 65 (1988) 1593.
- [16] G. Joshi, S. Deshpande, S.R. Sawant, J. Phys. A61 (1987) 241.
- [17] M.N. Kahn, A.A. Ahmad, V.S. Darshane, J. Mater. Sci. 24 (1989) 163.
- [18] R.B. Jootania, R.V. Upadhyay, P.G. Kulkarni, IEEE Trans. on Magn. 28 (1992) 1889.
- [19] C. Koops, Phys. Rev. 83 (1951) 121.
- [20] H.G. Zhang, L.T. Li, J. Zhou, J. Am. Ceram. Soc. 85 (5) (2002) 1180–1184.